crystals

MDPI

Article

Hot-Pressed Two-Dimensional Amorphous Metals and Their Electronic Properties

Jieying Liu [1,2], Jian Tang [1,2], Jiaojiao Zhao [1,2], Yanchong Zhao [1,2], Cheng Shen [1,2], Mengzhou Liao [1,2], Shuopei Wang [3], Jinpeng Tian [1,2], Yanbang Chu [1,2], Jiawei Li [1,2], Zheng Wei [1,2], Gen Long [3,*], Wei Yang [1,2,4], Rong Yang [1,3,4], Na Li [1,3,*], Dongxia Shi [1,2,4] and Guangyu Zhang [1,2,3,4,*]

[1] Beijing National Laboratory for Condensed Matter Physics, Key Laboratory for Nanoscale Physics and Devices, Institute of Physics, Chinese Academy of Sciences, Beijing 100190, China; jyliu@iphy.ac.cn (J.L.); jtang@iphy.ac.cn (J.T.); jiaojiaozhao@iphy.ac.cn (J.Z.); ychzhao@iphy.ac.cn (Y.Z.); cshen@iphy.ac.cn (C.S.); mzliao@iphy.ac.cn (M.L.); jptian@iphy.ac.cn (J.T.); ybchu@iphy.ac.cn (Y.C.); jiaweili@iphy.ac.cn (J.L.); zhengwei@iphy.ac.cn (Z.W.); wei.yang@iphy.ac.cn (W.Y.); ryang@iphy.ac.cn (R.Y.); dxshi@iphy.ac.cn (D.S.)

[2] School of Physical Sciences, University of Chinese Academy of Sciences, Beijing 100190, China

[3] Songshan Lake Materials Laboratory, Dongguan, Guangdong Province 523808, China; spwang@iphy.ac.cn

[4] Beijing Key Laboratory for Nanomaterials and Nanodevices, Beijing 100190, China

* Correspondence: longgen@sslab.org.cn (G.L.); nli@iphy.ac.cn (N.L.); gyzhang@iphy.ac.cn (G.Z.); Tel.: +86-10-8264-9021(G.Z.)

Citation: Liu, J.; Tang, J.; Zhao, J.; Zhao, Y.; Shen, C.; Liao, M.; Wang, S.; Tian, J.; Chu, Y.; Li, J.; et al. Hot-Pressed Two-Dimensional Amorphous Metals and Their Electronic Properties. *Crystals* **2022**, *12*, 616. https://doi.org/10.3390/cryst12050616

Academic Editor(s): Yao Yao, Giuseppe Greco

Received: 14 March 2022

Accepted: 22 April 2022

Published: 26 April 2022

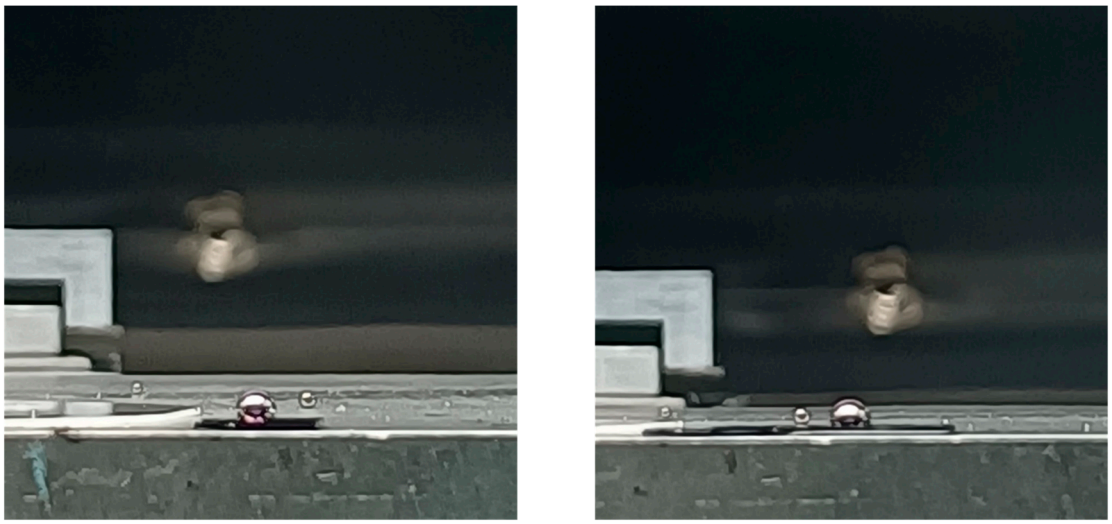

Figure S1. The contact angle between liquid bismuth drops and SiO_2(300nm)/Si substrate without (left) and with (right) O_2 plasma treatment.

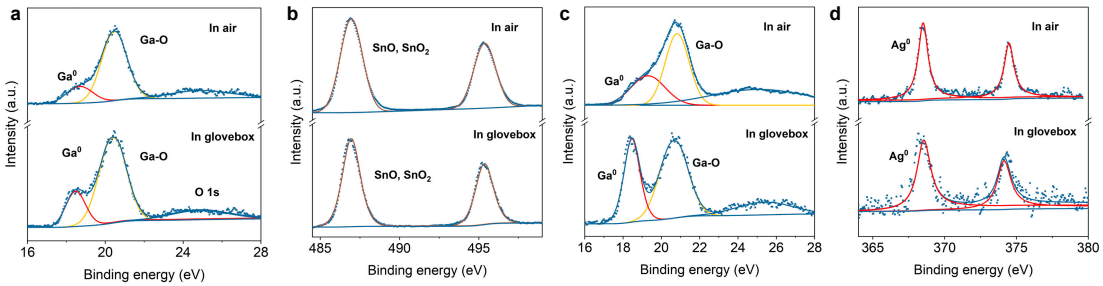

Figure S2. XPS spectra of (a) Ga 3d from Ga films, (b) Sn 3d from Sn films, (c) Ga 3d and (d) Ag 3d from $Ga_{0.87}Ag_{0.13}$ alloy films made in air (top panel) and in glovebox (bottom panel).

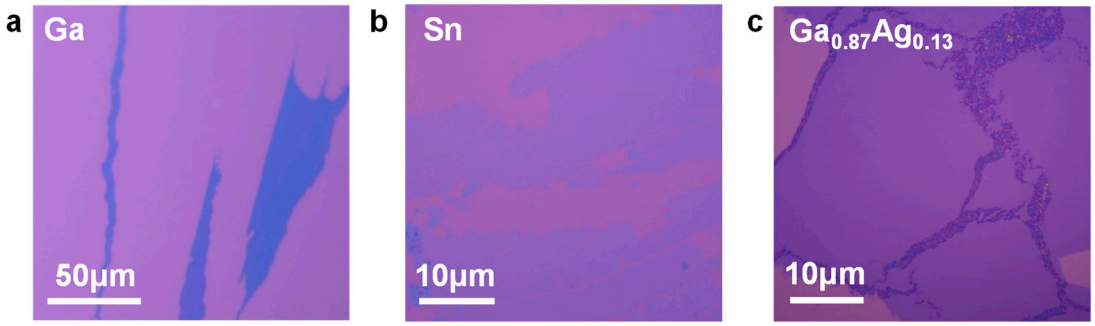

Figure S3. Optical images of 2D films made of Ga, Sn, and $Ga_{0.87}Ag_{0.13}$ alloy in glovebox.

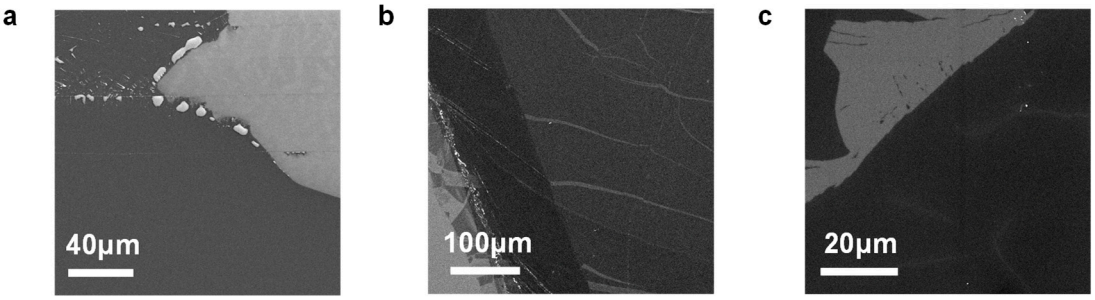

Figure S4. SEM images of 2D films made of Ga, Sn, and $Ga_{0.87}Ag_{0.13}$ alloy synthesized in glovebox.

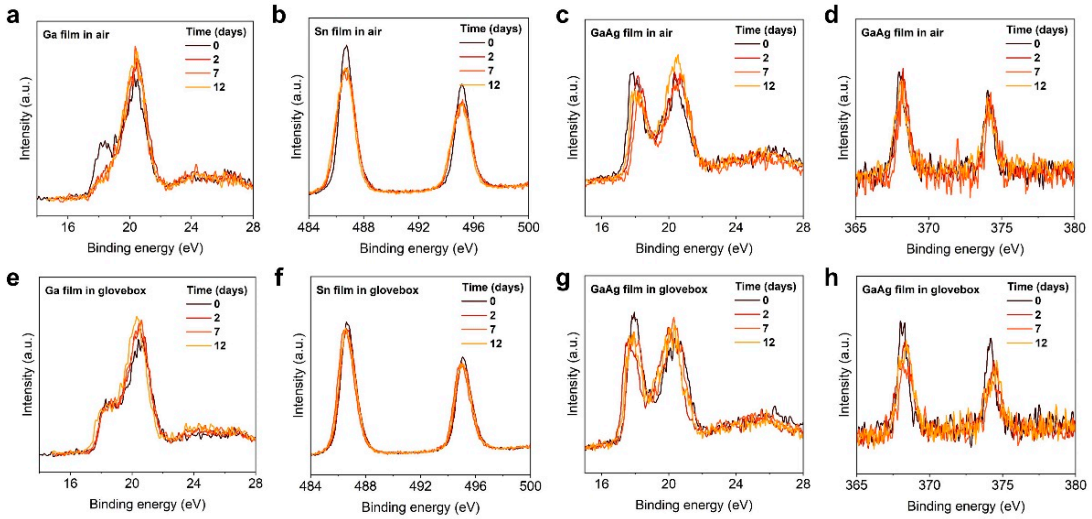

Figure S5. The variation of XPS spectrum of films made in glovebox and then stored in air and in glovebox for 12 days. (a, e) XPS of Ga 3d from Ga films stored in air (a) and in glovebox (e); (b, f) XPS of In 3d from In films stored in air (b) and in glovebox (f); (c, g) XPS of Ga 3d from $Ga_{0.87}Ag_{0.13}$ films stored in air (c) and in glovebox (g); (d, h) XPS of Ag 3d from $Ga_{0.87}Ag_{0.13}$ films stored in air (d) and in glovebox (h).

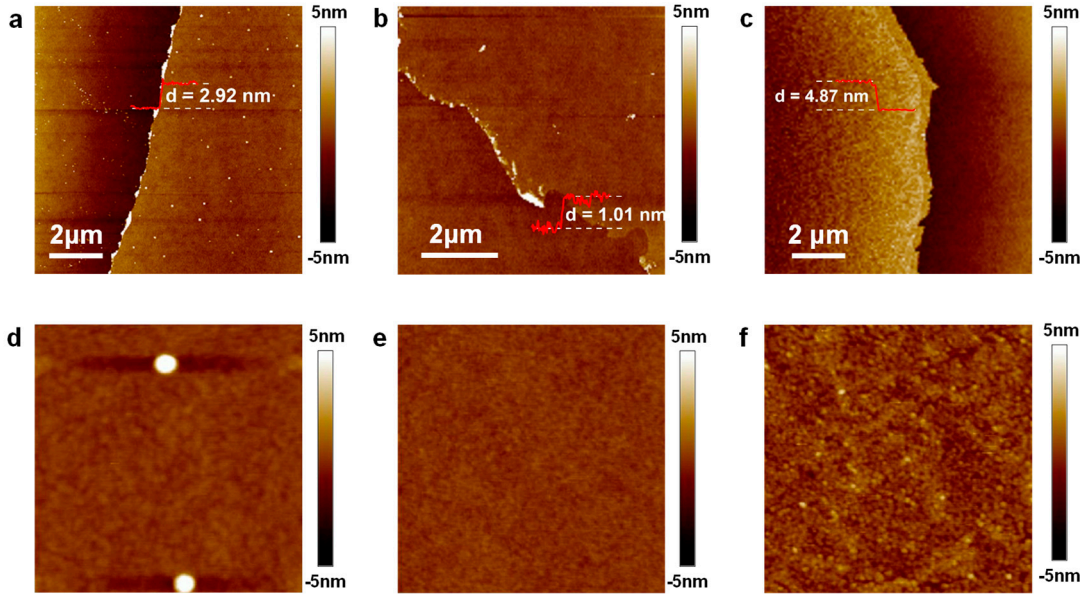

Figure S6. AFM images of 2D films made of (a, d) Ga, (b, e) Sn, and (c, f) $Ga_{0.87}Ag_{0.13}$ alloy. (a-c) show the thickness of films. (d-f) show the roughness of films, image width is 1um.

The Raman spectrum of hot-pressed metal films are presented below. As for Ga films and $Ga_{0.87}Ag_{0.13}$ films, according to previous studies [1, 2], solid crystalline gallium and β-Ga2O3 have characteristic Raman peaks at 246 cm-1 and 416 cm-1 The Raman spectrum of our Ga film (Figure S7a) and $Ga_{0.87}Ag_{0.13}$ film (Figure S7d) show no additional peaks compared to the Raman spectrum of substrate, indicating the absence of either crystalline metal gallium or crystalline Ga_2O_3. As for In films, previous study [3] demonstrates both rhombohedral and body-centered cubic In_2O_3 have multiple Raman active modes. The Raman spectrum of our In film (Figure S7b) shows no additional peaks compared to the Raman spectrum of substrate, indicating the absence of crystalline In_2O_3.As for Sn films, both crystal SnO_2 [4] and SnO [5] have characteristic Raman peaks. The Raman spectrum of our Sn film shows no additional peaks compared to the Raman spectrum of substrate, indicating the absence of any crystalline SnO and SnO_2.

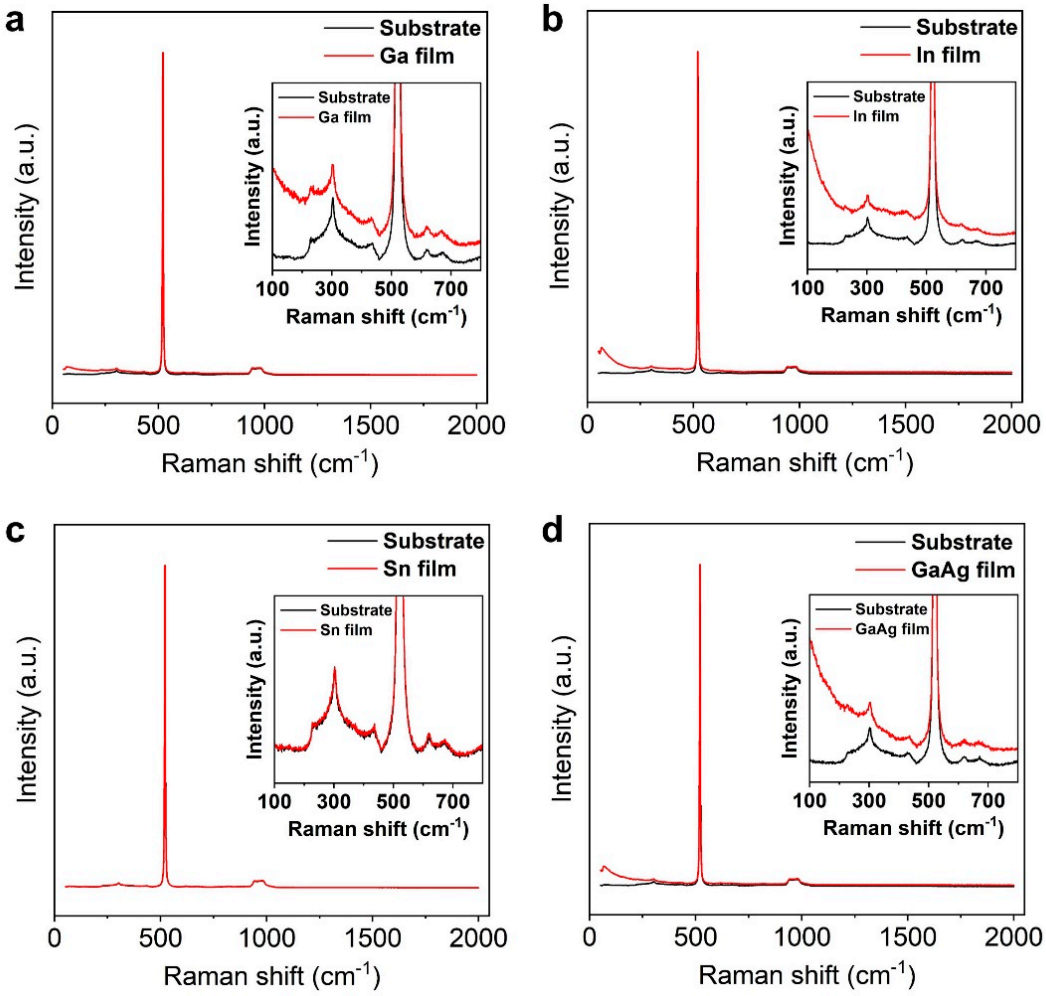

Figure S7. Raman spectrum of 2D films made of (a) Ga, (b) In, (c) Sn and (d) $Ga_{0.87}Ag_{0.13}$ alloy. Insets show the details of the Raman spectrum.

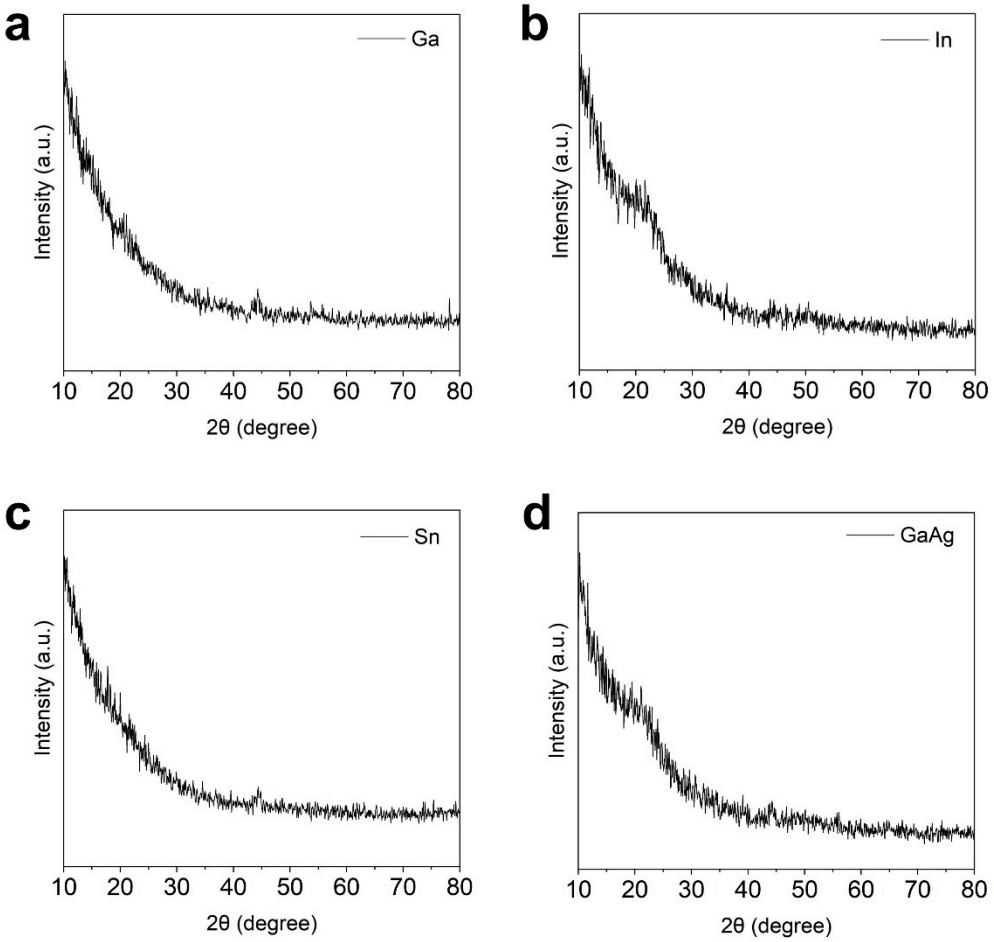

Figure S8. XRD spectra of (a) Ga film, (b) In film, (c) Sn film, (d) $Ga_{0.87}Ag_{0.13}$ alloy film.

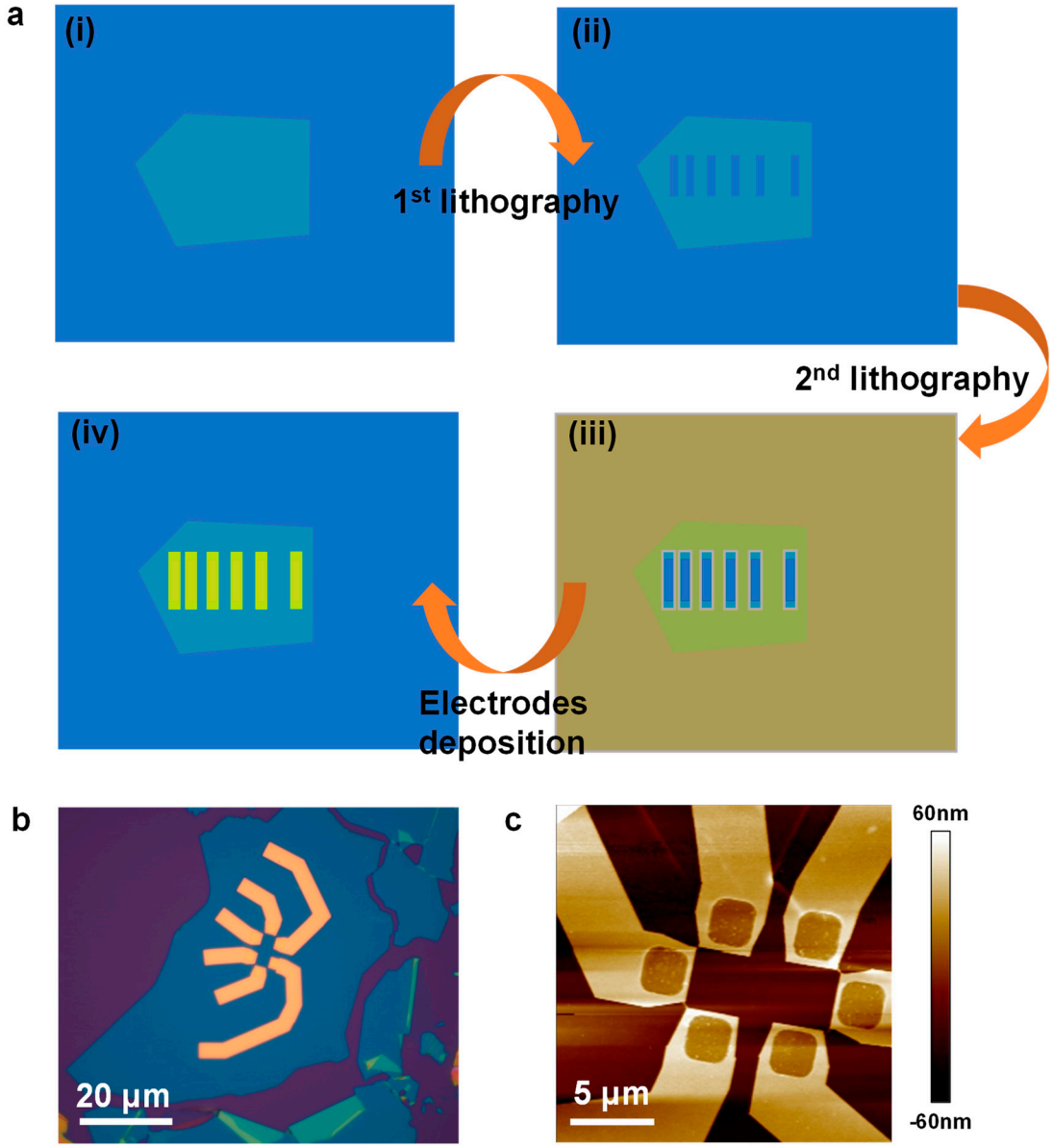

Figure S9. Fabrication process of h-BN-encapsulated electrodes. (a) Schematic of fabrication procedure of h-BN-encapsulated electrodes: (i) exfoliating h-BN on SiO_2 (300nm)/Si substrate, (ii) first pattern of contact voids on h-BN by EBL lithography and RIE etching, (iii) second lithography of gold electrodes, (iv) electron-beam evaporation of gold electrode. (b) Optical image of h-BN-encapsulated electrodes. (c) AFM image of h-BN-encapsulated electrodes.

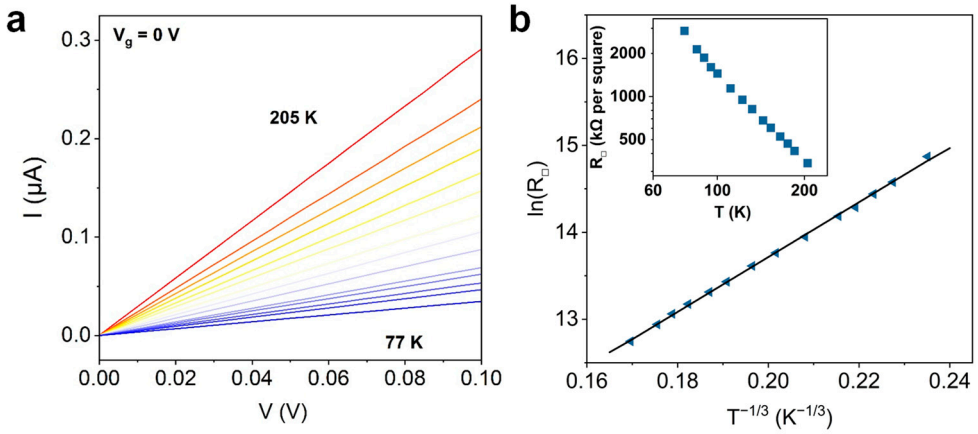

Figure S10. Electronic properties of Ga film. (a) I versus V curves as a function of temperature showing ohmic contact. (b) The sheet resistance $R_{\square}$ versus T fitted by 2D Mott's VRH model, inset is double-logarithmic plot of $R_{\square}$ versus T.

References:

1. Creighton, J.A.; Withnall, R. The Raman Spectrum of Gallium Metal. *Chemical Physics Letters* **2000**, *326*, 311–313, doi:10.1016/S0009-2614(00)00782-X.
2. Kranert, C.; Sturm, C.; Schmidt-Grund, R.; Grundmann, M. Raman Tensor Elements of β-Ga2O3. *Sci Rep* **2016**, *6*, 35964, doi:10.1038/srep35964.
3. Wang, Ch.Y.; Dai, Y.; Pezoldt, J.; Lu, B.; Kups, Th.; Cimalla, V.; Ambacher, O. Phase Stabilization and Phonon Properties of Single Crystalline Rhombohedral Indium Oxide. *Crystal Growth & Design* **2008**, *8*, 1257–1260, doi:10.1021/cg700910n.
4. Zhang, G.; Liu, N.; Ren, Z.; Yang, B. Synthesis of High-Purity SnO 2 Nanobelts by Using Exothermic Reaction. *Journal of Nanomaterials* **2011**, *2011*, 1–5, doi:10.1155/2011/526094.
5. Liu, Q.; Liang, L.; Cao, H.; Luo, H.; Zhang, H.; Li, J.; Li, X.; Deng, F. Tunable Crystallographic Grain Orientation and Raman Fingerprints of Polycrystalline SnO Thin Films. *J. Mater. Chem. C* **2015**, *3*, 1077–1081, doi:10.1039/C4TC02184C.